

ELASTIC IMPEDANCE STUDY IN RIP AREA, GULF OF THAILAND

Penprapa Wutthijuk

Department of Geology, Faculty of Science,
Chulalongkorn University, Bangkok, 10330, Thailand
Corresponding author email: penprapa_eay728@hotmail.com

Abstract

The predictions of fluvial sandstones deposited early to late Middle Miocene age, which are the main reservoirs in Pattani Basin, are always challenging. The well log data from 4 development wells and 2 exploration wells were applied with the partial-angle stacked seismic data in order to do elastic impedance inversion. Based on the rock physics analysis, the P-wave velocity does not show a good contrast for sands and shale while the density shows a significant contrast for these lithologies at all depth intervals. P-impedance shows good separation of sands and shales at the shallow section and has limitation of lithology discrimination at depth below 2000m. The crossplots of elastic impedances (near, mid and far) indicate that these can be used for lithology prediction. The far-angle elastic impedance is the best for lithology prediction and can also be used to identify the thick hydrocarbon sands in lower Middle Miocene age. The elastic impedance inversion successfully detects sands at all depths. Far-angle elastic impedance inversion effectively predicted thick hydrocarbon sands in the main reservoir interval. The elastic impedance inversion also shows good results in the case of blind-test for those wells which were not used in the inversion process. Its horizon slice successfully images the sand geometries associated with the proved reservoir distributions.

Key words: Elastic impedance, Inversion, Partial-angle stacked seismic

1. Introduction

The geophysical expectations in hydrocarbon reservoir exploration and evaluation are to predict or image its distribution and analyze the size and quality of reservoirs. The reservoirs in the study area are fluvial sands, which have limited lateral extent and normal faulting. Therefore, potential reservoir prediction in this area is always a challenge. Moreover, the limitations of full-stacked seismic data are the possibility of real geological data being removed during the seismic processing. The effort to recover information regarding incidence angles and P-wave, S-wave through the elastic impedance inversion may improve the understanding of the reservoir properties particularly lithology and fluid content (Zhou et al., 2009).

The study area is the RIP area in the western margin of central Pattani Basin, Gulf of Thailand (Figure 1). The previous study was focused on modeling the AVO attributes of this study area by using the near- and mid-angle stacked seismic data because the far-angle stacked seismic are not aligned with other two partial-angle stacked seismic that might be the effect of low frequency content (Punglusamee, 2014). Another study done in this area is the density inversion that the density prediction through simultaneous inversion. This gave a reasonable match with the sand distribution throughout the zone of interest (Ahmad and Rowell, 2013). Due to the variation of the elastic properties, the seismic response of the same reflected point might represent by the different seismic character at different incidence angles. In this study, I applied the

elastic impedance inversion at near-, mid- and far-angle in order to discriminate the lithology and fluid in the study area.

2. Objectives

The objectives of this thesis are to improve the imaging of reservoir distribution and enhance the discrimination of lithology and fluid within the reservoirs by using the elastic impedance inversion.

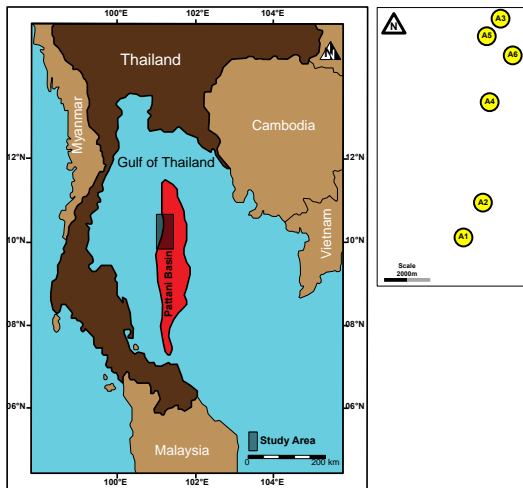


Figure 1. Map shows the location of the study area called RIP located in Gulf of Thailand.

Study Area

The study area is a part of Pattani Basin, a part of Gulf of Thailand that covers the area of 1300 km². It composes of several petroleum fields that sandstones are the major reservoirs and gas is the main hydrocarbon product. The basin is the Tertiary age that contains more than 7000 meters thickness of mainly non-marine fluvial deltaic sediments. The stratigraphy of this area was divided into 5 stratigraphic sequences (Figure 2) based on the depositional environments (Morley and Racey, 2011). The main reservoirs are sandstones deposited during the post-rift period that covered the sequence 2, 3 and 4 as shows in the Figure 2. Most of reservoir sands are stacked point bar sandstones with limited lateral distribution and compartmentalized by faults. The depth of reservoir interval ranges from 1400 to 2700 meters below mean sea level and the thickness of individual reservoir sandstone ranges from 2 to 20 meters. The hydrocarbon

type is mainly gas with some oil. The reservoirs are both hydrocarbon full to base and hydrocarbon-water contact.

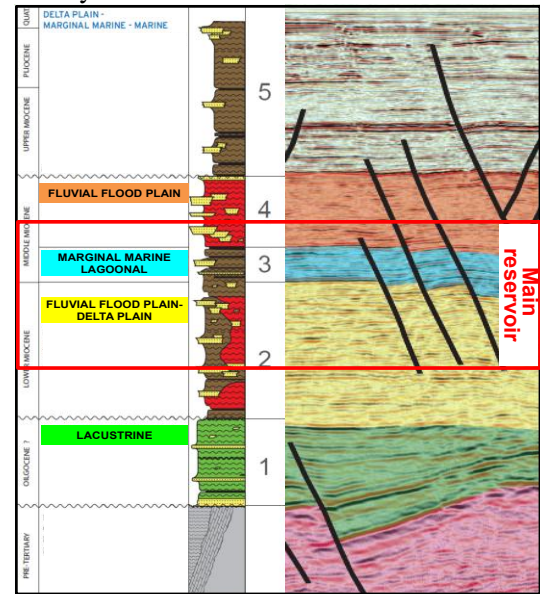


Figure 2. Regional stratigraphy and depositional environment of the Gulf of Thailand (Morley and Racey, 2011).

Data Sets

Well Log Data

There are six drilled wells located in the study area. The well log data of all six wells were used for rock physics analysis. The original well log data consist of gamma ray, density, resistivity, neutron porosity, P-wave velocity, S-wave velocity and checkshot data.

Seismic Data

The 3D seismic data which covers 1300 km² of the study area, are full-stacked seismic data, and three partial-angle stacked seismic data. The seismic was shot at 3000 km length lines and then had AVO reprocessing. The partial-angle stacked seismic data are near-, mid- and far-angle stacked seismic data. The near-angle stacked seismic data comprises the reflected seismic wave ranges from 5° to 22° incidence angle. The mid-angle stacked seismic data is the stack of reflected seismic wave ranges from 18° to 35° incidence angle. The far-angle stacked seismic data consists of reflected seismic wave ranges from 36° to 60° incidence angle.

3. Methodology

Rock physics analysis and seismic inversion are two main methods that were used to discriminate sands from shales and detect the sand distribution. The result and interpretation from rock physics analysis is to understand the character of each rock property along the well including the target zone intervals and to decide which rock physics properties can best differentiate the lithology.

Rock Physics Analysis

Several crossplots were done including density, P-wave velocity, S-wave velocity, P-impedance, S-impedance and elastic impedances. The crossplots were analyzed to check the depth dependence of rock physical parameters such as P-wave velocity, S-wave velocity and density with respect to gamma ray value, shale volume and water saturation. The P-wave velocity and density were used to combine with the extracted wavelet in order to calculate the P-impedance and generate the zero-offset synthetic traces.

The elastic impedance of different reflected angles were computed using relationship of P-wave velocity (V_p), S-wave velocity (V_s) and density (ρ) in the Connolly's equation (Connolly, 1999).

$$EI(\theta) = V_p^a V_s^b \rho^c \quad (1)$$

$$\begin{aligned} \text{where} \quad a &= 1 + \tan^2(\theta) \\ b &= -8K \sin^2(\theta) \\ c &= 1 - 4K \sin^2(\theta) \end{aligned}$$

θ is the incident angle and K is the ration of V_p and V_s

Computing the elastic impedance needs the input value of reflected angle, so the middle value of each partial-angle stacked seismic was used to compute the near (14°), mid (27°) and far (47°) angle elastic impedances. The original well log data were up scaled to 4 milliseconds, which is the seismic scale to compare with the inversion output at the same vertical resolution.

Inversion

The elastic impedance relates to the elastic properties of subsurface geology and responses in seismic survey in term of P-wave velocity (V_p), S-wave velocity (V_s) and density (ρ). In case that the incident angle

(θ) is not zero, the situation becomes more complicated due to mode conversion between P-wave and S-wave. The elastic properties in this case can be described by using Shuey's equation (Shuey, 1985).

$$R(\theta) = R(0) + G \sin^2(\theta) + F \tan^2(\theta) \sin^2(\theta) \quad (2)$$

$$\begin{aligned} \text{where } R(0) &= \frac{1}{2} \left(-\frac{\Delta V_p}{V_p} + \frac{\Delta \rho}{\rho} \right) \\ G &= \frac{1}{2} \frac{\Delta V_p}{V_p} - \frac{2V_s^2}{V_p^2} \left(\frac{\Delta \rho}{\rho} + \frac{2\Delta V_s}{V_s} \right) \\ F &= \frac{1}{2} \frac{\Delta V_p}{V_p} \end{aligned}$$

Base on the Shuey's equation as show above, the second and third terms become more dominate when the angle is greater. Therefore, the far-angle stacked seismic information commonly contains more information of subsurface elastic properties and might be useful in order to discriminate the lithology or fluid.

The simultaneous inversions were performed using near (5° - 22°), mid (18° - 35°) and far (36° - 60°) partial-angle stacked seismic data. The first step of the inversion process is to complete the well to seismic ties that link the well data to seismic data. Then, the initial geological models of elastic impedance and density were created for near, mid and far partial-angle stacked seismic data using the well log data, computed elastic impedance, extracted wavelet and interpreted horizons within the target intervals. Due to the limitation of low frequency band in seismic data, the 5-10 Hz frequency was used to create the initial models.

The two methods applied to invert the seismic data, are the model-based method and colored inversion method. The model-based method is mainly to invert seismic data based on the well log data and interpolate the seismic data between wells. Therefore, this method will give more accurate result in the study area with many drilled wells. The colored inversion method is another inversion method that focuses on the seismic data only (Purisa, 2014). The elastic impedance inversion results were compared with the original logs for quality control at both wells that used to create the inversion models and blind-test wells, with

those wells which were not used in the inversion process.

4. Results

Rock Physics Analysis

The crossplots (Figure 3) of density and P-wave velocity versus depth with respect to shale volume indicate the strong dependence of the lithology to density. The density of sands is significantly lower than shales and the density contrast can be used to isolate sands from shales at all depths. The crossplot of P-wave velocity versus depth with respect to shale volume shows that the P-wave velocity is not only dependent on the lithology but also dependent on depth.

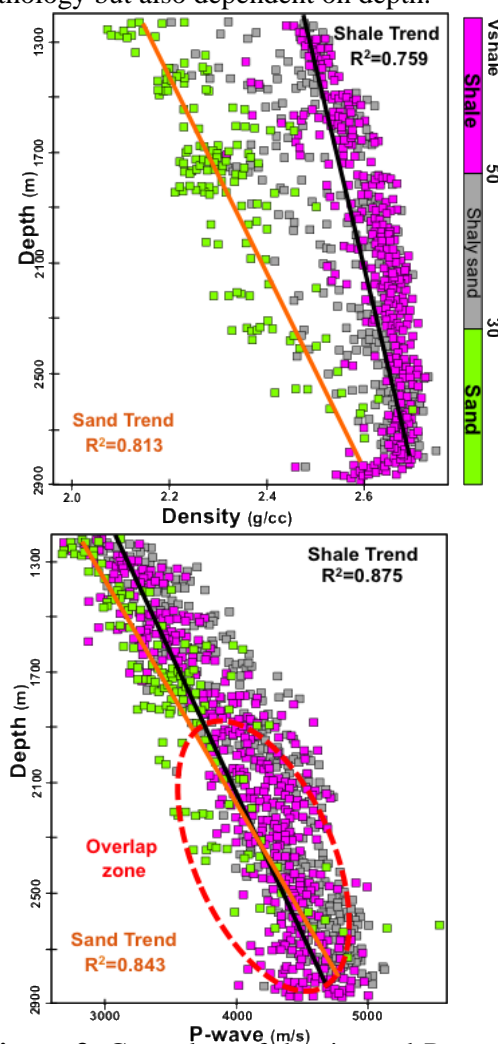


Figure 3. Crossplots of density and P-wave velocity versus depth colored code by shale volume.

The P-wave velocity of sands is lower than shales down to 2100 meters. Below that

depth, the P-wave velocity of sands is similar to shales and the crossover trend was found at depths below 2500 meters. Therefore, the P-wave velocity can be used to discriminate sands from shales clearly in sequence 4 and shallow part of sequence 3. Also, in this depth interval sands have lower density and P-wave velocity than shales, and these properties refer to the P-impedance contrasts to be useful to discriminate sands from shales in this depth interval.

The crossplot (Figure 4) of P-impedance versus depth with respect to shale volume shows clearly separated trends of sands and shales for the whole interval. Due to the decreasing of P-wave velocity contrast below 2100 meters, the P-impedance contrast of sands shales decreases with depth.

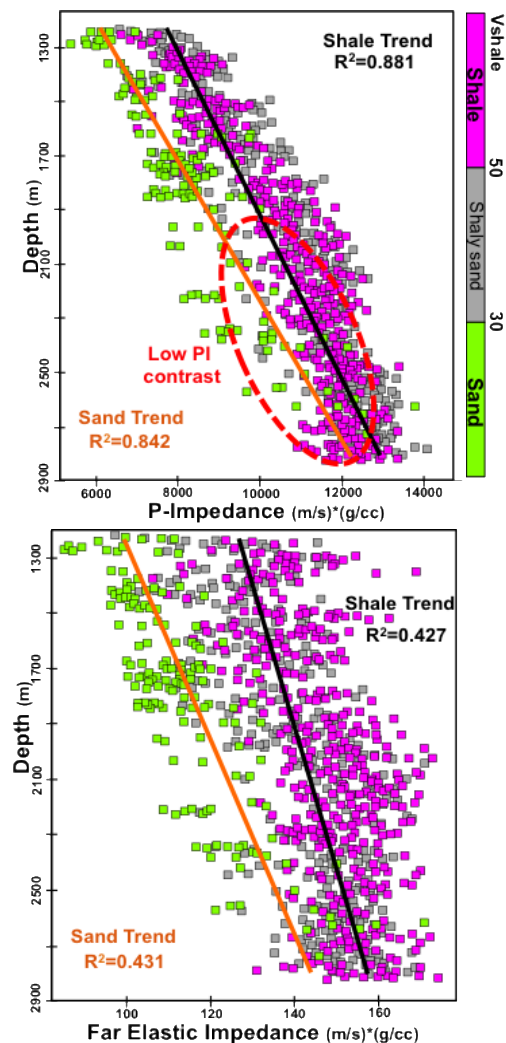


Figure 4. Crossplots of P-impedance and far elastic impedance versus depth colored code by shale volume.

The results of crossplots in Figure 4 indicate that full-stacked seismic data that solve only for P-impedance contrast will be useful to discriminate the lithology clearly in the shallow stratigraphic sequence down to deeper part of sequence 3 (2000 meters). Below that depth the full-stacked seismic data will have the limited lithology discrimination in the study area. On the other hand, at all depth intervals sands and shales have larger contrast of far-angle elastic impedance as compared to P-impedance. Therefore, the far-angle elastic impedance

inversion technique will be useful to differentiate the sands from shales at all depths in the study area.

The crossplot (Figure 5) of gamma ray and density with respect to stratigraphic sequences indicates a clearly separation of sands and shales. The gamma ray cut off for sand is lower than 90 API. The shaded area covers 90-150 API on the crossplot represents the zone of silty shale and shaly sand. The P-wave velocity crossplot with respect to gamma ray shows increasing of P-wave velocity with depth.

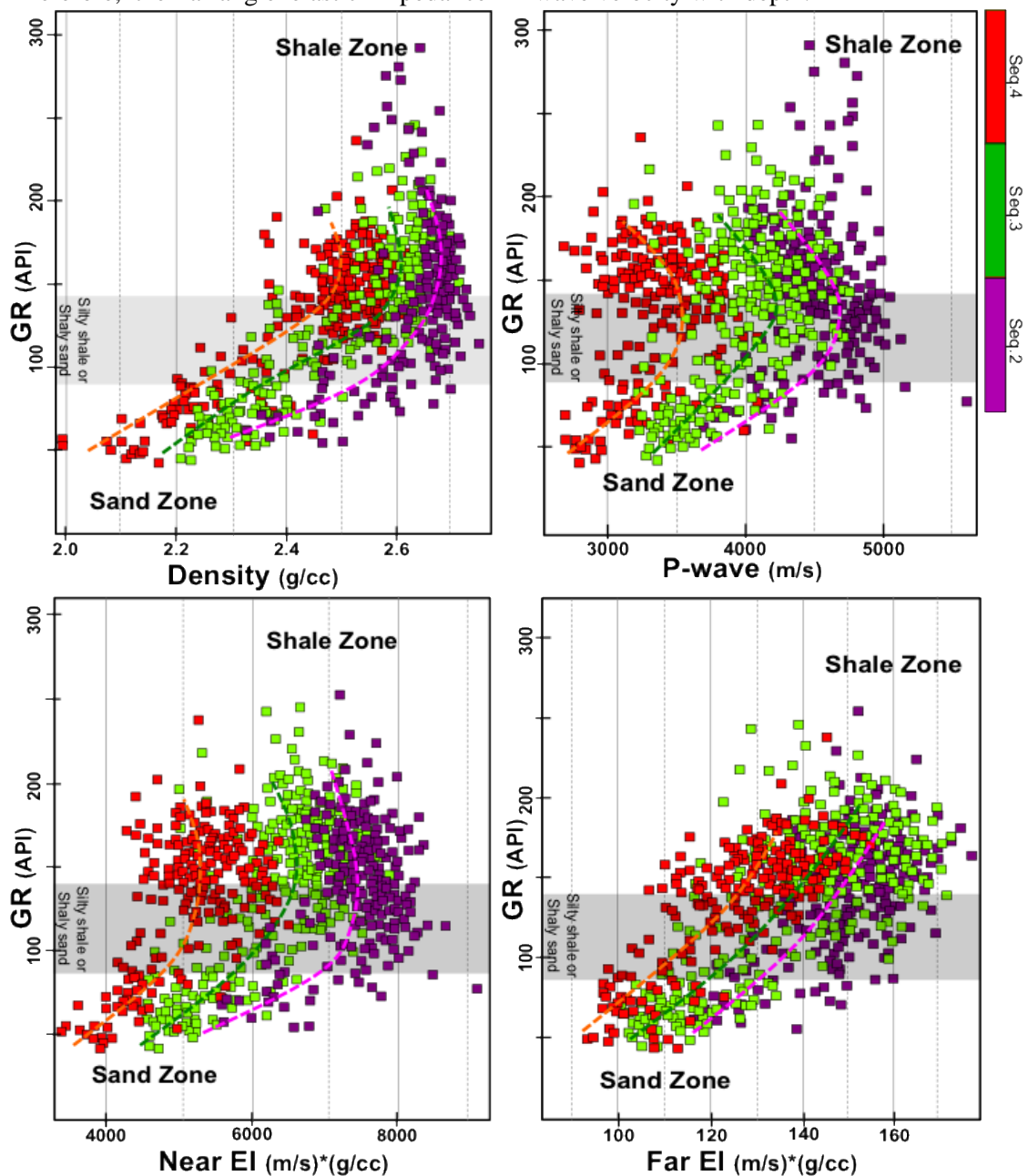


Figure 5. Crossplots of density, P-wave velocity, near and far elastic impedance versus gamma ray colored code by stratigraphic sequences.

However, there are several overlap zones of sands and shales P-wave velocity in the same stratigraphic sequence. The elastic impedance crossplots (Figure 5) show the increasing of elastic impedance values with depth but the same overlap zones of sands and shales are found in near-angle elastic impedance crossplot. Within the same stratigraphic sequence, the far-angle elastic impedance shows clear separation trends of sands and shales. The far-angle elastic impedance crossplot shows the linear relationship between these two parameters stronger than the results to density crossplot. This implies that the far-angle elastic impedance inversion technique would be more suitable for lithology discrimination at all stratigraphic sequences.

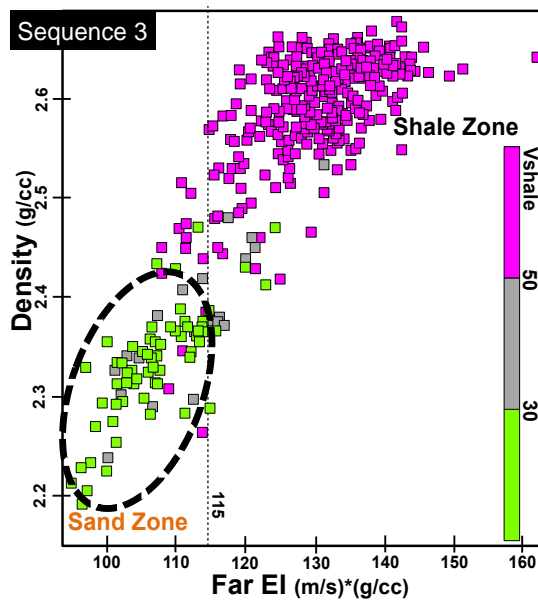


Figure 6. Crossplot of far-angle elastic impedance versus density colored code by shale volume of the main reservoir section.

The elastic impedances of near-, mid- and far-angle of each stratigraphic sequence were plotted separately with respect to shale volume. The crossplots (Figure 6) of far-angle elastic impedance show the significant contrast of sands and shales in all stratigraphic sequences. The cutoff value between sands and shales using far-angle elastic impedance is 125 (m/s)*(g/cc) in sequence 3.

The crossplot (Figure 7) of far-angle elastic impedance with respect to water

saturation indicates clearly different trends of hydrocarbon and wet sands found in sequence 3. The cutoff value of fluid is 90-100 (m/s)*(g/cc) based on far-angle elastic impedance.

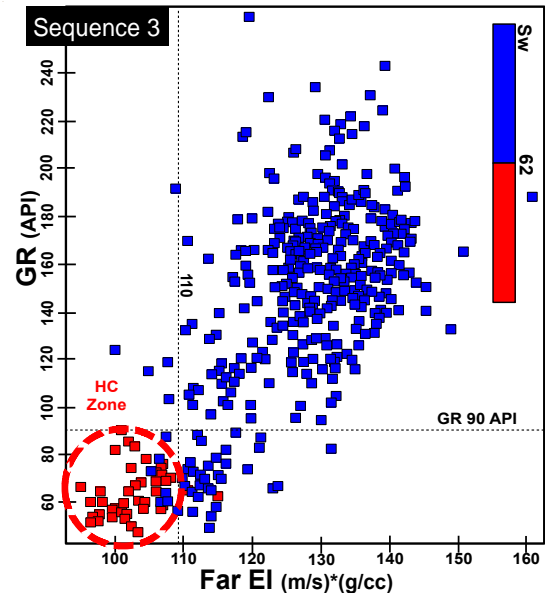


Figure 7. Crossplots of far-angle elastic impedance versus gamma ray colored code by water saturation of the main reservoir section.

Inversion

The near, mid, and far-angle elastic impedance inversion models were created by using the model-based inversion method and colored inversion method. Each model was analyzed with computed elastic impedance log and the correlation coefficient ranges from 0.641 to 0.929.

The elastic impedance of sands are lower than shales. The far-angle elastic impedances of sands range from 110 to 125 (m/s)*(g/cc) which is represented by green to orange colors (Figure 8). Figure 8a shows the conformable results of far angle elastic impedance inversions at the wells, which were used to build the inversion model, with the well log interpretation. Figure 8b also shows good results in blind-tests for those wells, which were not used in the inversion process. Moreover, most of the hydrocarbon sands shown in Figure 8 are represented by green colored code, which refers to 90-100 (m/s)*(g/cc) far angle elastic impedance.

The seismic inversion from model-based method show good results at the well locations and the resolution decreases when distance increases. The colored inversion method shows better results for all areas than model based method.

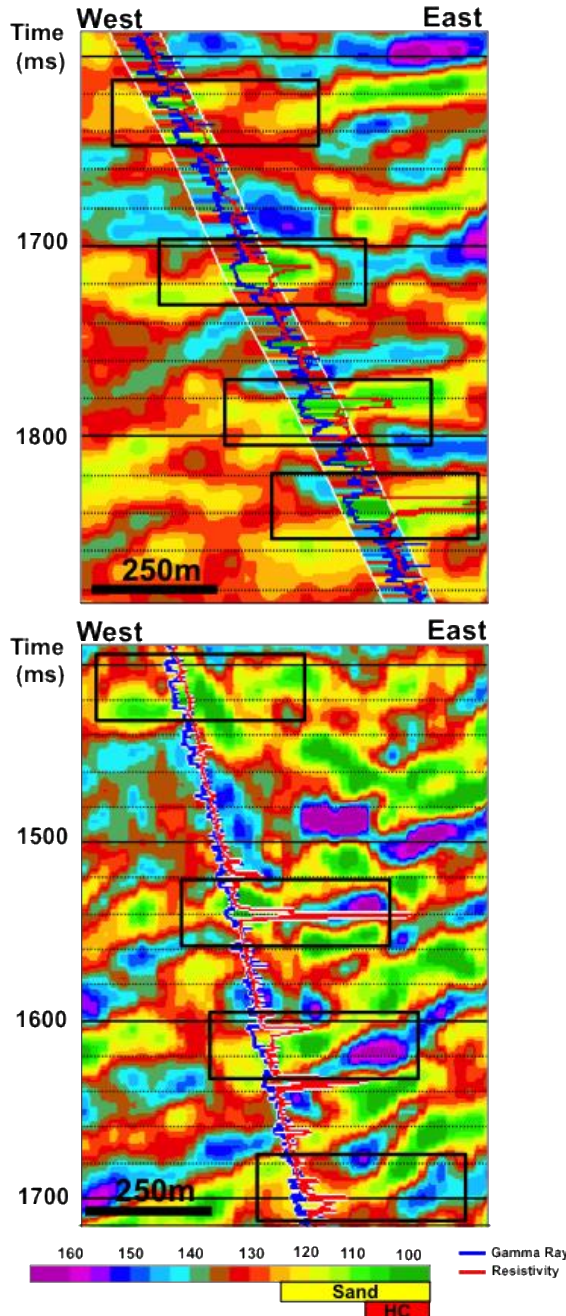


Figure 8. Far-angle elastic impedance inversion sections of well used in inversion process (upper figure) and blind-test well (lower figure).

The seismic crossplots were done to see the relationship of near- and mid-angle

elastic impedance inversion, near- and far-angle elastic impedance inversion and mid- and far-angle elastic impedance inversion with respect to shale volume and water saturation. The selected zones were based on well log crossplots and were applied to seismic crossplots and the same points were selected on the inverted vertical sections along blind-test wells, which were not used in the inversion process (Figure 9 and 10). The lithology color coded on the far-angle elastic impedance inversion section represents the conformable result to well log interpretation (Figure 9). Therefore, the far-angle elastic impedance inversion can be used to discriminate the lithology in all sequences. The far-angle elastic impedance crossplot with respect to water saturation shows good fluids identification in the case of thick hydrocarbon sands as shown by red color-coded in far-angle elastic impedance inversion section (Figure 10).

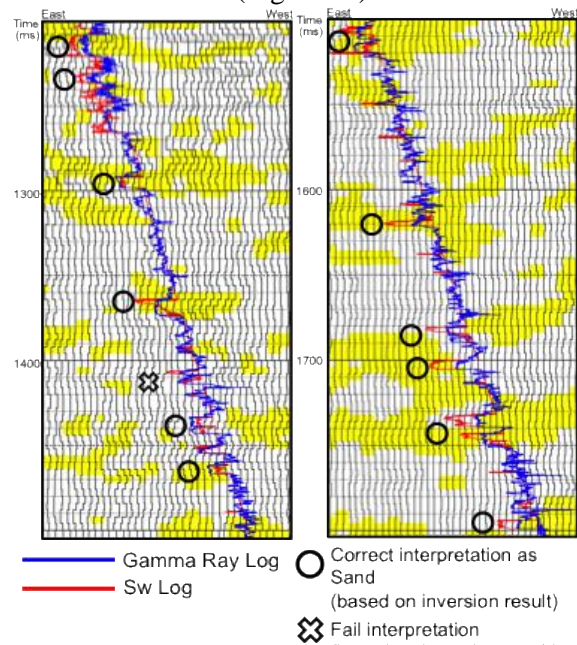


Figure 9. Far-angle elastic impedance inversion sections at blind-test well colored code by predicted sand zones (yellow zones).

The crossplot analysis based on both rock physics results and inverted seismic results indicated that far-angle elastic impedance could best discriminate sands from shales and also predict the fluid for the main reservoir interval.

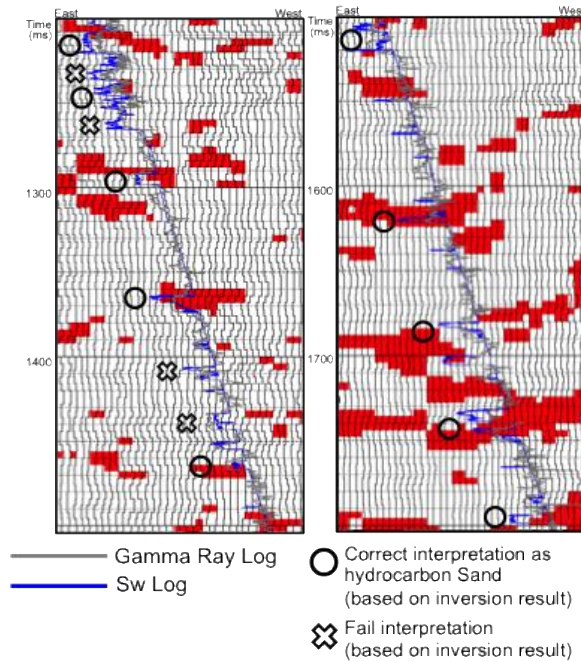


Figure 10. Far elastic impedance inversion sections at blind-test well colored code by predicted hydrocarbon zones (red zones).

The horizon slice within the far-angle elastic impedance inversion volume was analyzed and it indicated the geological channel-like feature of sand distribution (Figure 11 and 12).

Based on the results of rock physics crossplot and inverted seismic observation, the lower values than $125 \text{ (m/s)} \cdot \text{(g/cc)}$ of far-angle elastic impedance, represent sands. Moreover, most of values less than $100 \text{ (m/s)} \cdot \text{(g/cc)}$ of far-angle elastic impedance represent hydrocarbon sands. The large red-yellow body in Figure 11 represents the clear trend of sand distribution and the circles represent the proved results of blind-test wells from well log data. There are 2 wells, which penetrated at the red zones found the hydrocarbon sands while other 7 wells, which penetrated at the green zones found wet sands. In Figure 11, there are large areas represented by the orange and yellow colors indicating potential hydrocarbon filled channel sands, which have not yet been tested. Therefore, using the far-angle elastic impedance inversion and horizon slices could provide useful information about the lithology discrimination and reservoir distribution in order to reduce the exploration and development risks.

Figure 12 shows similar result to figure 11 that far-angle elastic impedance inversion successfully images the hydrocarbon bearing.

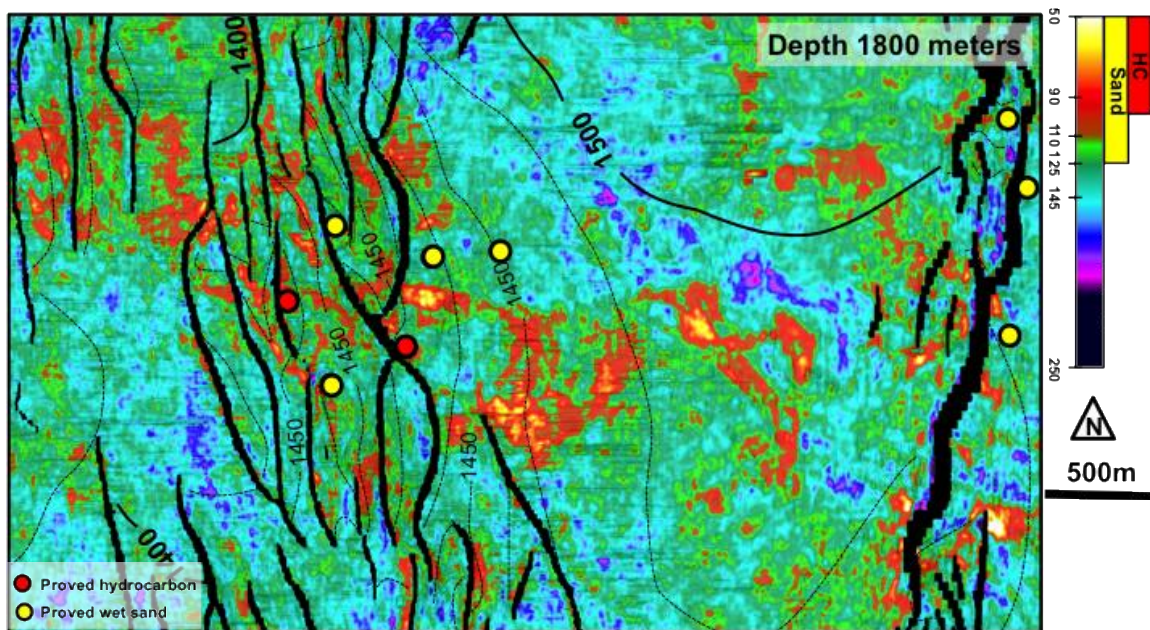


Figure 11 Horizon slice at 1800 meters from the far elastic impedance inversion volume with the several blind-test wells. Seven drilled wells (yellow circles) found wet sands and two drilled wells (red circle) found hydrocarbon sands.

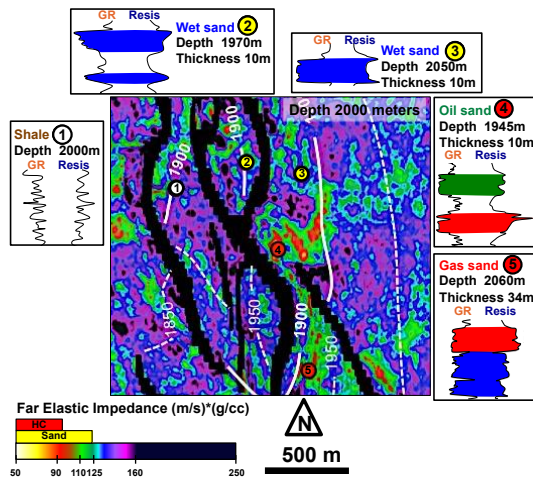


Figure 12 Horizon slice at 2000 meters from the far elastic impedance inversion volume with the several blind-test drilled wells.

5. Discussion

There are three important results found in this thesis that point out the significant benefits of using far offset seismic information. All three points are emphasized below.

1. Far-angle stacked seismic data contains more elastic properties than near-angle stacked seismic data or full-stacked seismic data. In the study area, the rock physics analysis show the difficulty of lithology discrimination in the deep section, including the main reservoir section, due to the similar value of P-wave velocity of sand and shale. Based on the rock physics, the elastic property that can be used to discriminate the different lithology along the well section (sequence 2, 3 and 4) is density. The increase of incident angle makes the density more dominant than near-angle stacked seismic information. Therefore, far-angle stacked seismic data of the study area can be used to discriminate the lithology along the whole section better than near angle or zero offset seismic data.

2. Far-angle stacked seismic data gives more reasonable channel belt character in several sand amplitude extracted maps. Due to large impedance contrast of sands and shales when the incident angle is greater, this significant contrast gives the clear channel like features in RMS amplitude-extracted map than near-angle stacked and full-stacked seismic data. The clear channel like features

can be used to relate to reservoir size prediction and possibly to reservoir connection identification and reservoir volume estimation.

3. Inversion of far-angle stacked seismic data proved a good technique to predict the lithology and fluid. Using the value of elastic impedances obtained from rock physics analysis, the sands can be discriminated from shales for all stratigraphic sequences. Moreover, the far-angle elastic impedance inversion can be used to identify the fluids in the main reservoir section. Far elastic impedance inversion technique successfully mapped the geological channel-like feature, which indicates the sand distribution and can be used for reservoir prediction in the interval of interest.

One possible reason of better lithology and fluid discrimination of far-angle elastic impedance inversion is related to the increasing of density contrast when the angle is greater. Based on Shuey's equation, the second and third term will be greater when the angle is greater. The second term contains the density value of each lithology. The dominant parameter of sands and shales discrimination in the study area is density. Therefore the increase of the incident angle relates to the increase in density contrast between sands and shales. This contrast may cause the significant contrast of far-angle elastic impedance and allow better discrimination of both lithology and fluid.

6. Conclusions

The elastic impedance study using the rock physics analysis, seismic observation and elastic impedance inversion has been done for a data set of RIP area, Gulf of Thailand. The key points proved by this thesis are listed as below.

- The density can be used to discriminate the lithology in all sequences while P-wave velocity shows some overlap zone of sands and shales within the same stratigraphy.
- P-impedance can differentiate the lithology clearly in sequence 4 and the top sands show as trough seismic characters (negative responses). In sequence 2 and 3, the P-impedance has limited lithology

discrimination capability due to the changing of P-wave velocity trends. Top sands found as peak seismic characters (positive responses) and zero contrasts in these two sequences.

- Far-angle elastic impedance can clearly differentiate between sands and shales throughout 3 stratigraphic sequences and can be used to isolate the hydrocarbon sands from wet sands in the main reservoir interval. Sands show low elastic impedance as compared to shales and hydrocarbon sands show lower elastic impedance than wet sands.
- Far-angle elastic impedance inversion provides a reasonable prediction of lithology and fluid in the main reservoir interval. It can be used to image the sand distributions and possibly to indicate the potential reservoir distributions.

Elastic impedance inversion using angle gathers can further improve the prediction of reservoir distribution and fluid type.

7. Acknowledgements

I would like to express my deep gratitude to my thesis supervisor Professor Angus John Ferguson for his patient guidance, enthusiastic encouragement and useful critiques of this research work. I also express my gratitude to Professor Naseer Ahmad for invaluable advice, encouragement, support, and guidance.

This thesis was made possible through academic and financial support from the Chevron Thailand Exploration and Production for the opportunity and scholarship for studying Master Degree of Petroleum Geoscience at Chulalongkorn University and their data support for this thesis.

8. References

Ahmad, M. N. and Rowell, P., 2013, Mapping of fluvial sand systems using rock physics analysis and simultaneous inversion for density: case study from Gulf of Thailand: *First break*, v. 31, May 2013, p. 49-54.

Connolly, P., 1999. Elastic impedance: The Leading Edge, v. 18, p. 438-452.

Morley, C.K., and Racey, A., 2011, Tertiary stratigraphy, in M.F. Ridd, A.J. Barber, and M.J. Crow, eds., *The geology of Thailand: Geological Society of London*, p. 223-271.

Punglusamee, K., 2014, AVO Feasibility study for hydrocarbon detection in northwestern of the Pattani basin, Gulf of Thailand: M.Sc. thesis, Chulalongkorn University, 67 p.

Purisa, W., 2014, Evaluation of post-stack seismic inversion techniques for detection of sands in the Gulf of Thailand: M.Sc. thesis, Chulalongkorn University, 54 p.

Shuey, R.T., 1985, A simplification of the Zoeppritz equations: *Geophysics*, v. 50, p. 609-614.

Zhou J. Y., Tao J. Q., Guo Y. B., Zhang X. H. and Qiang M., Rock Physics Based Pre-stack Seismic Reservoir Characterization-application to Thin Bed, 71th EAGE Conference and Exhibition, Amsterdam, The Netherlands, 8-11 June, 2009.